ORIGINAL ARTICLE

Journal of Cachexia, Sarcopenia and Muscle 2017; **8**: 926–938
Published online 28 August 2017 in Wiley Online Library (wileyonlinelibrary.com) **DOI:** 10.1002/jcsm.12232

Mitochondrial degeneration precedes the development of muscle atrophy in progression of cancer cachexia in tumour-bearing mice

Jacob L. Brown[1], Megan E. Rosa-Caldwell[1], David E. Lee[1], Thomas A. Blackwell[1], Lemuel A. Brown[2], Richard A. Perry[2], Wesley S. Haynie[2], Justin P. Hardee[3], James A. Carson[3], Michael P. Wiggs[4], Tyrone A. Washington[2] & Nicholas P. Greene[1]*

[1]*Integrative Muscle Metabolism Laboratory, Exercise Science Research Center, Department of Health, Human Performance and Recreation, University of Arkansas, Fayetteville, AR72701, USA;* [2]*Exercise Muscle Biology Laboratory, Exercise Science Research Center, Department of Health, Human Performance and Recreation, University of Arkansas, Fayetteville, AR72701, USA;* [3]*Integrative Muscle Biology Laboratory, Department of Exercise Science, University of South Carolina, Columbia, SC29208, USA;* [4]*Integrated Physiology and Nutrition Laboratory, Department of Health and Kinesiology, University of Texas at Tyler, Tyler, TX75799, USA*

Abstract

Background Cancer cachexia is largely irreversible, at least via nutritional means, and responsible for 20–40% of cancer-related deaths. Therefore, preventive measures are of primary importance; however, little is known about muscle perturbations prior to onset of cachexia. Cancer cachexia is associated with mitochondrial degeneration; yet, it remains to be determined if mitochondrial degeneration precedes muscle wasting in cancer cachexia. Therefore, our purpose was to determine if mitochondrial degeneration precedes cancer-induced muscle wasting in tumour-bearing mice.

Methods First, weight-stable (MinStable) and cachectic (MinCC) $Apc^{Min/+}$ mice were compared with C57Bl6/J controls for mRNA contents of mitochondrial quality regulators in quadriceps muscle. Next, Lewis lung carcinoma (LLC) cells or PBS (control) were injected into the hind flank of C57Bl6/J mice at 8 week age, and tumour allowed to develop for 1, 2, 3, or 4 weeks to examine time course of cachectic development. Succinate dehydrogenase stain was used to measure oxidative phenotype in tibialis anterior muscle. Mitochondrial quality and function were assessed using the reporter MitoTimer by transfection to flexor digitorum brevis and mitochondrial function/ROS emission in permeabilized adult myofibres from plantaris. RT-qPCR and immunoblot measured the expression of mitochondrial quality control and antioxidant proteins. Data were analysed by one-way ANOVA with Student–Newman–Kuels post hoc test.

Results MinStable mice displayed ~50% lower *Pgc-1α*, *Pparα*, and *Mfn2* compared with C57Bl6/J controls, whereas MinCC exhibited 10-fold greater *Bnip3* content compared with C57Bl6/J controls. In LLC, cachectic muscle loss was evident only at 4 weeks post-tumour implantation. Oxidative capacity and mitochondrial content decreased by ~40% 4 weeks post-tumour implantation. Mitochondrial function decreased by ~25% by 3 weeks after tumour implantation. Mitochondrial degeneration was evident by 2 week LLC compared with PBS control, indicated by MitoTimer red/green ratio and number of pure red puncta. Mitochondrial ROS production was elevated by ~50 to ~100% when compared with PBS at 1–3 weeks post-tumour implantation. Mitochondrial quality control was dysregulated throughout the progression of cancer cachexia in tumour-bearing mice. In contrast, antioxidant proteins were not altered in cachectic muscle wasting.

Conclusions Functional mitochondrial degeneration is evident in LLC tumour-bearing mice prior to muscle atrophy. Contents of mitochondrial quality regulators across $Apc^{Min/+}$ and LLC mice suggest impaired mitochondrial quality control as a commonality among pre-clinical models of cancer cachexia. Our data provide novel evidence for impaired mitochondrial health prior to cachectic muscle loss and provide a potential therapeutic target to prevent cancer cachexia.

Keywords Cancer; Cachexia; MitoTimer; ROS; Muscle wasting; Mitochondrial quality

Received: 18 April 2017; Revised: 16 June 2017; Accepted: 14 July 2017
**Correspondence to: Nicholas P. Greene, Exercise Science Research Center, University of Arkansas, 155 Stadium Dr, 321Q HPER, Fayetteville, AR 72701, USA. Phone: 479-575-6638. Fax: 479-575-2853. Email: npgreene@uark.edu*

Introduction

Cancer is one of the leading causes of death worldwide.[1,2] Moreover, therapies to prevent mortality from cancer are inadequate.[3] Cancer cachexia is a wasting syndrome that occurs in up to 80% of cancer cases and is directly attributable for up to 40% of cancer-related deaths.[4–6] Cancer cachexia is primarily defined by an ongoing loss of skeletal muscle mass and function, which nutritional therapies currently lack sufficient efficacy to reverse.[4,6] Therefore, prevention remains a substantial goal of cachexia research, and recent literature calls for a focus on therapies to prevent cachexia.[7] Prior evidence suggests that skeletal muscle oxidative capacity may influence atrophy in cancer cachexia and other forms of muscle wasting.[8–11] Mitochondria are organelles critical for muscle oxidative metabolism. In fact, mitochondrial quality may be critical to the maintenance of skeletal muscle mass.[12] We recently acquired evidence in *Apc*$^{Min/+}$ mice, a genetic model of colorectal cancer, suggesting impaired mitochondrial quality control in quadriceps muscle of weight-stable (not yet cachectic) mice (*Figure* 1). These data suggest that impaired mitochondrial quality may precede development of cachexia and thus be a critical step in the development of this condition, which has recently been discussed in detail.[13] Therefore, to better define such impacts, we have sought to investigate the development of mitochondrial impairments across a time course of cachectic development in tumour-bearing mice.

Mitochondrial quality can be defined as the general health and function of the mitochondrial network.[14] When the mitochondrial network is impaired, degeneration of the network structure occurs leading to a loss of mitochondrial function (impaired ATP production)[15] and excess mitochondrial reactive oxygen species (ROS) production, disrupting cellular health.[16,17] These related but distinct events result in impaired mitochondrial health and may initiate skeletal muscle atrophy.[18–24] Cancer appears to impair the mitochondrial network in skeletal muscle,[25] which may lead to cancer cachexia. In addition to mitochondrial degeneration in cancer cachexia, a decreased content of ROS-eliminating enzymes has been reported.[26] Antioxidants may attenuate the progression of cancer cachexia by aiding in the elimination of cellular ROS,[27] suggesting ROS as an instigator for cancer cachexia. Considering these points, there is a clear need to understand if mitochondrial degeneration, associated with mitochondrial ROS production and impaired energy production, may be the initiating event behind the onset of cancer cachexia.

Skeletal muscle has a series of processes involved in mitochondrial quality control to aid in the maintenance of the mitochondrial network.[14,28] These processes are the biogenesis of new mitochondrial components, fusion and fission of new and damaged mitochondrial regions within the network (dynamics), and the selective degradation of damaged mitochondrial regions through the process of autophagy (mitophagy).[28] Mitochondrial biogenesis is primarily regulated by PGC-1α, a transcriptional co-activator that coordinates the transcription factors critical for the addition of mitochondrial components.[29] Mitochondrial dynamics is a highly regulated process in which components of the mitochondrial network are enzymatically divided (fission) or merged (fusion).[28] Mitophagy is a highly selective engulfment of mitochondria by autophagosomes and their subsequent catabolism by lysosomes.[30,31] Many of these mitochondrial regulatory processes are impaired in cancer cachectic muscle,[13,25,32] which may directly promote skeletal muscle atrophy[33–35]; however, current literature predominantly only measures mitochondrial quality control regulators at late-

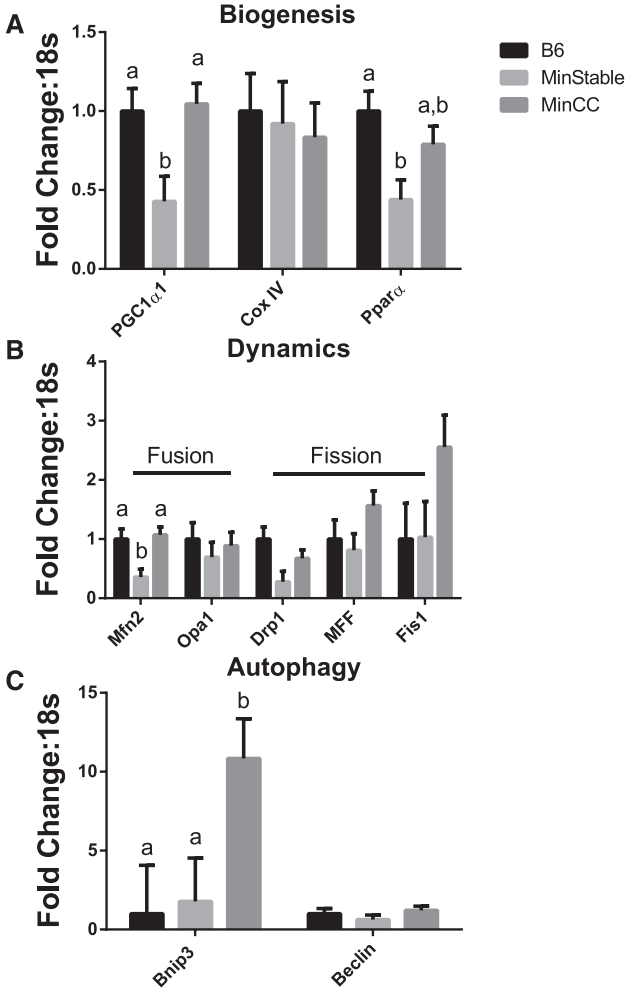

Figure 1 mRNA content of mitochondrial quality controllers in quadriceps muscle of B6 and APC/Min^{+} mice. (A) mRNA content of mitochondrial biogenesis controllers. (B) mRNA content of mitochondrial dynamic controllers. (C) mRNA content of mitophagy regulators. *N* of 5–6 was utilized for each group. Lettering denotes statistical significance at an alpha set at $P < 0.05$.

DOI: 10.1002/jcsm.12232

stage cancer cachexia. It is possible that this mitochondrial degeneration occurs only after development of cancer-induced muscle wasting; however, currently, it is not known if such mitochondrial degeneration may precede and potentially instigate the muscle wasting in cancer cachexia.

To our knowledge, mitochondrial degeneration during the progression of cancer cachexia has not been examined over a time course protocol; therefore, the purpose of this study was to examine mitochondrial quality throughout the progression of cancer cachexia in tumour-bearing mice. We hypothesized that impaired mitochondrial quality would be evident prior to the onset of cachexia. To test this hypothesis, we measured multiple functional (ROS emission, respiratory function, degeneration via pMitoTimer reporter gene) and signalling aspects of the mitochondria across time course progression of cancer cachexia in tumour-bearing mice. Utilizing direct and functional measurements of the mitochondrial network over time course progression, we now highlight a potential mechanism behind the onset of cancer cachexia. We additionally provide evidence that signalling for mitochondrial quality control is impaired in pre-cachectic mice from each of two pre-clinical models of cancer cachexia. Our study provides a novel insight into mitochondrial perturbations prior to development of the cachectic phenotype.

Methods

Animals and interventions

Animal experiments were performed at two major institutions. All procedures were approved by the Institutional Animal Care and Use Committees of the University of Arkansas, Fayetteville [Lewis lung carcinoma (LLC) experiments] and University of South Carolina ($Apc^{Min/+}$ experiments). A subset of the mice used for the LLC experiment has previously been reported on.[36]

In the current study, we have utilized two pre-clinical models of cancer cachexia—the $Apc^{Min/+}$ mouse, a genetic model of colorectal cancer, and LLC implantation. Initial observations were made at the level of mRNA contents in the $Apc^{Min/+}$ and followed by functional assessments of mitochondrial quality through time course of tumour development using the LLC implantation model. As pre-clinical models of cancer cachexia often exhibit inherent differences, the utilization of two models additionally was utilized to add surety that observations were not unique to any one model.

$Apc^{Min/+}$ mice

$Apc^{Min/+}$ mice used in this study were on a C57BL/6 (B6) background and were originally purchased from Jackson Laboratories. All mice used in the present study were obtained from the investigator's breeding colony (JAC) within the Center for Colon Cancer Research Mouse Core at the University of South Carolina. Experimental mice were group housed, kept on a 12:12 h light–dark cycle, and had access to standard rodent chow (No. 8604 Rodent Diet; Harlan Teklad, Madison, WI) and water *ad libitum*. Male $Apc^{Min/+}$ and B6 mice were aged to 18–20 weeks of age and stratified based on cachexia severity at sacrifice as previously described.[25] Experimental groups included [B6 (control)], weight-stable $Apc^{Min/+}$ mice (MinStable; no weight loss), and cachectic $Apc^{Min/+}$ mice (MinCC; 11.3% body weight loss). Phenotypic description of $Apc^{Min/+}$ mice is shown in *Table* 1.

Lewis lung carcinoma growth and tumour implantation

Lewis lung carcinoma cells (ATCC CRL-1642) were plated in 250 mL culture flasks in DMEM supplemented with 10% foetal bovine serum plus 1% penicillin and streptomycin. Once confluent, cells were trypsinized, counted, and diluted in PBS for implantation. LLC cells were plated at passage 2.

Male C57BL/6J (stock 000664) mice were purchased from Jackson Laboratories. The mice were kept on a 12:12 h light–dark cycle with *ad libitum* access to normal rodent chow and water. At 6 weeks of age, MitoTimer[15] (a reporter gene that directly measures mitochondrial quality) was delivered by electric pulse-mediated gene transfer to the flexor digitorum brevis (FDB) muscle on one foot of each mouse (described in the succeeding texts). LLC cells (1×10^6) suspended in 100 μL sterile PBS were implanted to the hind flank of mice at 8 weeks of age as described.[36,37] The tumour was allowed to develop for 1, 2, 3, or 4 weeks in separate cohorts of animals. For sham control, one group of mice received a bolus injection of 100 μL sterile PBS. PBS controls were age-matched to the most cachectic group (4 weeks post-implantation, 12 weeks of age at tissue collection). Animal tissues were quickly collected under isoflurane anaesthesia prior to euthanasia. Tissues were weighed and snap-frozen in liquid nitrogen for further processing and stored

Table 1 Body and tissue weights in B6 and $Apc^{Min/+}$ mice

Variable	B6	MinStable	MinCC
Peak BW (g)	27.4 ± 0.4	25.34 ± 0.7	25.5 ± 0.9
Sac BW (g)	27.4 ± 0.4 a	25.34 ± 0.7 a	22.7 ± 0.8 b
BW loss (g)	0 ± 0 a	0 ± 0 a	11.3 ± 1.1 b
Quadriceps (mg)	111.7 ± 4.7 a	103.5 ± 3.1 a	67 ± 5.5 b
Tibia (mm)	17.5 ± 0.1	17.06 ± 0.1	17.2 ± 0.1

Tibia length was measured as an estimate of total body size which did not differ between experimental groups; therefore, all tissue weights are presented as non-normalized wet weights. Lettering denotes statistical significance at an alpha set at $P < 0.05$.

at −80°C. Body weights between the PBS and 4 week group were not different; however, the 4 week group lost a significant amount of muscle mass. According to Fearon *et al*., loss of skeletal muscle mass is an effective diagnostic criterion for cancer cachexia.[6] Phenotypic description of LLC tumour-bearing mice is shown in *Table* 2.

Plasmid DNA amplification and electroporation

DH5-α *Escherichia coli* containing pMitoTimer plasmid[15] were amplified and plasmid DNA isolated using PureLink HiPure Plasmid Filter Maxiprep kit (Life Technologies, K210017). Plasmid transfection to FDB muscle was performed as described by Laker *et al*.[15] Briefly, 10 μL of 0.36 mg/mL hyaluronidase (in saline) was injected with insulin syringe with a 30 gauge needle subcutaneously above the FDB muscle prior to plasmid DNA injection. One hour after hyaluronidase injection, 20 μg of DNA was injected into the FDB muscle. Ten minutes following DNA injection, the mice were anesthetized, and an electrical field was delivered through gold-plated acupuncture needles placed at the heel of the foot and at the base of the toes. Ten pulses were delivered at 20 ms duration/pulse and 1 Hz at 75 V using an S88 stimulator (Grass Telefactor).

Mitochondrial function and ROS production

This methodology was adapted from Min *et al*.[38] Briefly, small strips of plantaris muscle, ~10 mg, were teased to near-single fibres and permeabilized with saponin to open small pores in the membrane. Mitochondrial oxygen consumption (VO_2) of a permeabilized fibre bundle was measured. Briefly, mitochondria were primed with malate and glutamate. Maximal respiration (ADP-stimulated, state 3) and state 4 respiration (ADP-depleted respiration) were measured. The respiratory control ratio (RCR) was calculated by dividing state 3 by state 4 respiration. The dry weight of the permeabilized mitochondria was used to normalize the results.

Mitochondrial ROS was measured in permeabilized plantaris fibres. All forms of ROS were converted to hydrogen peroxide by the addition of superoxide dismutase 1. ROS emission was measured using Amplex Red Hydrogen Peroxide Detection Kit. In the presence of peroxidase, the Amplex Red reagent reacts with H_2O_2 in a 1:1 stoichiometry to produce the red fluorescent oxidation product, resorufin. Plantaris muscle was utilized for mitochondrial respiration and ROS analyses because it is a mixed fibre type and as a smaller muscle more easily teased apart into near single fibre bundles, which is required for the assay.

Fluorescence microscopy for MitoTimer

For MitoTimer, freshly harvested FDB muscles were fixed for 20 min in 4% paraformaldehyde at room temperature and washed 5 min in PBS. Muscles were then whole mounted on gelatin-coated glass slides using 50% glycerol in PBS as mounting media and cover slipped. MitoTimer images were acquired at ×100 magnification using the FITC (green, excitation/emission 488/518 nm) and TRITC (red, excitation/emission 543/572 nm) channels on a Nikon Ti-S inverted epiflourescent microscope (Melville, NY) with LED-based light source with controlled acquisition parameters as described by Laker *et al*.[15] All slides were imaged the day of tissue harvest. Acquisition parameters were set using a pilot study of cachectic and control animals and maintained consistent throughout all experiments. A specially written MATLAB program was a generous gift from Dr Z. Yan (U. Virginia) and was used to analyse MitoTimer red:green ratio and pure red puncta as described by Laker *et al*.[15] The assay is best performed on freshly dissected muscles as time *ex vivo*

Table 2 Body and tissue weights at the time of harvest in Lewis lung carcinoma tumour-bearing mice

Variable (LLC)	PBS (N = 24)	1 week (N = 16)	2 weeks (N = 16)	3 weeks (N = 12)	4 weeks (N = 14)
Body weight (g)	24.9 ± 0.3 a	23.9 ± 0.3 a	23.8 ± 0.6 a	24.4 ± 0.8 a	27.0 ± 0.6 b
Tumour weight (g)	N/A	0.03 ± 0.007 a	0.2 ± 0.03 a	0.8 ± 0.1 b	3.5 ± 0.4 c
BW—tumour (g)	24.9 ± 0.3	23.9 ± 0.3	23.7 ± 0.6	23.6 ± 0.7	23.5 ± 0.6
TA (mg)	45.1 ± 0.9 a	43.8 ± 1.2 a	44.5 ± 1.2 a	42.9 ± 1.6 a	38.3 ± 1.3 b
Gastroc (mg)	134.6 ± 2.1 a	129.5 ± 2.5 a	130.0 ± 4.1 a	125.2 ± 3.5 a,b	118.4 ± 4.1 b
Plantaris (mg)	18.3 ± 0.4 a	18.3 ± 0.3 a	18.1 ± 0.6 a	17.7 ± 0.7 a	15.9 ± 0.6 b
EDL (mg)	9.9 ± 0.4	9.4 ± 0.3	9.9 ± 0.3	9.6 ± 0.4	8.6 ± 0.5
Soleus (mg)	8.7 ± 0.2 a	8.2 ± 0.2 a,b	8.1 ± 0.2 a,b	8.1 ± 0.3 a,b	7.7 ± 0.2 b
Spleen (mg)	81.1 ± 3.2 a	81.9 ± 2.8 a	85.7 ± 2.6 a	222.8 ± 31.1 b	366.5 ± 31.8 c
Lungs (mg)	151.2 ± 6.8	173.0 ± 8.9	161.7 ± 3.9	173.2 ± 8.9	156.8 ± 10.0
EpiFat (mg)	367.5 ± 12.9 a	332.5 ± 22.6 a	348.2 ± 12.8 a	316.7 ± 33.6 a	240.4 ± 19.2 b
Quadriceps (mg)	152.3 ± 6.7	149.2 ± 5.7	147.8 ± 8.8	148.5 ± 7.6	127.1 ± 7.2
Tibia (mm)	17.4 ± 0.1	17.4 ± 0.1	17.3 ± 0.1	17.4 ± 0.1	17.3 ± 0.1

N of 12–24/group as indicated on table was utilized. Tibia length was measured as an estimate of total body size which did not differ between experimental groups; therefore, all tissue weights are presented as non-normalized wet weights. Lettering denotes statistical significance at an alpha set at $P < 0.05$.

impacts the fluorescent indicator of MitoTimer. Therefore, we transfected and utilized the FDB which can be dissected, whole mounted to microscope slide, and imaged within 30 min of the initial dissection.

Cryosectioning

Tibialis anterior (TA) muscles were embedded in optimal cutting temperature compound and frozen in liquid nitrogen-cooled isopentane. Sections were cut at 10 μm using a Leica CM1859 cryostat (Leica Biosystems, Buffalo Grove, IL) and stained for succinate dehydrogenase (SDH). Sections were placed in incubation solution (50 mM sodium succinate, 50 mM phosphate buffer, 0.12 M KH_2PO_4, and 0.88 M Na_2HPO_4), 0.5 mg/mL nitroblue tetrazolium for 40 min in a 37°C water bath. Slides were washed 3 min with dH_2O and imaged. Images were collected with Nikon Sight DS-Vi1 camera mounted on an Olympus CKX41 inverted microscope. SDH+ (purple) and SDH– fibres were counted, cross-validated by two independent and blinded investigators, and circled for cross-sectional area (CSA) analysis using Nikon Basic Research Imaging Software (Melville, NY). There was no difference between the measurements across two blinded researchers. TA muscle was utilized because it is a bigger muscle, which minimizes freezer damage to fibres to centrally located muscle fibres. Other muscles suitable for cryosectioning such as the gastrocnemius were utilized for other analyses.

RNA isolation, cDNA synthesis, and quantitative real-time PCR

RNA isolation, cDNA synthesis, and quantitative real-time PCR were performed as we have previously described.[14,39–41] Taqman probes or SYBR primers specific to *Pgc-1α1*, *Cox4*, *Pparα*, *Mfn2*, *Opa1*, *Drp1*, *MFF*, *Fis1*, *Bnip3*, and *Beclin1.* Taqman probes and SYBR primers have previously been reported in Greene *et al*.[14]

Immunoblotting

Immunoblotting performed as we have previously described.[14,40–43] Membranes were probed overnight for primary antibodies. Protein targets were selected based upon prior literature to encompass key components of each of the mitochondrial quality control systems[14,28] and ROS protection[26,44] as previously described. Primary antibodies were specific to mitochondrial content and biogenesis proteins: COX-IV (Cell Signalling 4844S), VDAC (Cell Signalling 4866S), PGC-1α (Santa Cruz sc-13067), PPARα (Santa Cruz sc-9000), PPARδ (Santa Cruz sc-7197), and TFAM (Cell Signalling 7495). Mitochondrial dynamics proteins: MFN1 (Santa Cruz sc-50330), MFN2 (Santa Cruz sc-50331), OPA1 (Santa Cruz sc-367890), DRP1 (Cell Signalling 14647), and Fis1 (Novus NB100-56646). Mitophagy proteins: BNIP3 (Cell Signalling 3769), PINK 1 (Santa Cruz sc-33796), p-PARKIN (Ser65, Abcam ab154995), and PARKIN (Cell Signalling 42115). Antioxidant proteins: SOD1 (Genetex GTX100554), SOD2 (Cell Signalling 131945), SOD3 (R and D Systems AF4817), GPx7 (Genetex GTX117516), GPx3 (Genetex GTX89142), and catalase (Cell Signalling 140975). Primary antibodies were isolated from rabbit, mouse, and goat. Antibodies were diluted in Tris-buffered saline, 0.1% Tween 20 with 5% milk. Membranes were imaged on Protein Simple FluorChem (Minneapolis, MN) and analysed using Alpha View software. All bands were normalized to the 45 kDa actin band of Ponceau S stain as a loading control. There was no difference detected between the 45 kDa actin band of Ponceau S stain across experimental groups. Powdered gastrocnemius muscle (mixed fibre type) was utilized to represent both type I and II fibres for immunoblot analysis.

Statistical analysis

For $Apc^{Min/+}$, independent variables were B6 control, weight-stable $Apc^{Min/+}$ mice (MinStable), and cachectic $Apc^{Min/+}$ mice (MinCC). For LLC, independent variables were PBS and number of weeks tumour progressed. A one-way ANOVA was employed as the global analysis for each dependent variable in both experiments. Differences among means were determined by Student–Newman–Keuls post hoc test. For all experiments, the comparison-wise error rate, α, was set at 0.05 for all statistical tests. All data were analysed using the Statistical Analysis System (SAS, version 9.3, Cary, NC, USA); figures were compiled using GraphPad Prism (La Jolla, CA, USA) and data expressed as mean ± standard error of the mean.

Results

Mitochondrial quality control is dysregulated before severe cancer cachexia in $Apc^{Min/+}$ mice

$Apc^{Min/+}$ mice were stratified into experimental groups based on % total body weight loss from peak body weight as an estimate of cachectic development as previously described.[25] Cachectic mice (MinCC) lost on average 11.3% body weight by time of tissue harvest, while no loss was seen in B6 or weight-stable (MinStable) controls (*Table* 1). Loss of body weight coincided with reduction in quadriceps muscle mass. While no significant differences in muscle mass were observed between B6 (118 ± 4.6) and MinStable (103 ± 3.6), MinCC (67 ± 5.5) quadriceps mass was reduced compared

DOI: 10.1002/jcsm.12232

with both B6 and MinStable (*Table* 1). Intriguingly, the process of mitochondrial biogenesis was dysregulated in MinStable mice indicated by a ~50% decrease in mRNA content of both *Pgc-1α* and *Pparα* (*Figure* 1A). Furthermore, a ~50% decrease in *Mfn2* mRNA in weight-stable $Apc^{Min/+}$mice indicated alterations in mitochondrial fusion before cancer cachexia occurred (*Figure* 1B). *Bnip3* mRNA was increased by 10-fold in MinCC only, which indicates an up-regulation of mitophagy in mice with cancer cachexia (*Figure* 1C).

Characterization of the progression of Lewis lung carcinoma-induced cancer cachexia

Body weights (body weight with tumour weight subtracted) of the C57Bl/6J mice were not different between groups throughout the 4 week progression of cancer cachexia; however, muscle wet weights of TA, gastrocnemius, plantaris, quadriceps, and soleus were ~15–20% lower 4 weeks following tumour implantation compared with PBS, with no significant differences in muscle weights between PBS, 1, 2, and 3 week animals (*Table* 2). Furthermore, epididymal fat decreased by ~35% in mice with 4 weeks tumour growth compared with PBS. Spleen weight, a surrogate marker for inflammatory state, was 270 and 450% greater 3 and 4 weeks, respectively, following tumour implantation when compared with PBS control (*Table* 2).

Oxidative phenotype is diminished 4 weeks following tumour implantation

The percentage of SDH+ fibres in the TA muscle was ~20% lower in mice 4 weeks following tumour implantation (*Figure* 2A and 2B), indicating a loss of muscle oxidative phenotype. Furthermore, there was a greater number of small muscle fibres that are SDH− 4 weeks following tumour implantation compared with PBS control, while little difference was observed in SDH+ suggesting specific atrophy of non-oxidative muscle fibres (*Figure* 2C and 2D). There was a lower mitochondrial content 4 weeks following tumour implantation compared with PBS indicated by a ~50% decrease in both COX-IV and VDAC protein contents (*Figure* 2E–G). No significant changes in SDH or mitochondrial content (COX-IV/VDAC) were observed prior to 4 week tumour development.

Figure 2 Oxidative muscle fibres and mitochondrial content across a time course progression of cancer cachexia in Lewis lung carcinoma tumour-bearing mice. (A–D) SDH staining performed in TA muscle. (A) Representative images for SDH stain across the different experimental groups. Scale bar is 50 μM long. (B) % SDH+ fibres throughout the progression of cancer cachexia. (C) Cross-sectional area distribution of SDH+ fibres. (D) Cross-sectional area distribution of SDH− fibres. (E–G) Immunoblotting in gastrocnemius muscle. (E) and (F) Immunoblot quantification of mitochondrial content markers COX-IV (E) and VDAC (G). (G) Representative immunoblot images. *N* of 10 for each group was used for SDH analysis, and *N* of 8 for each group was utilized for immunoblot analysis. Lettering denotes statistical significance at an alpha set at $P < 0.05$.

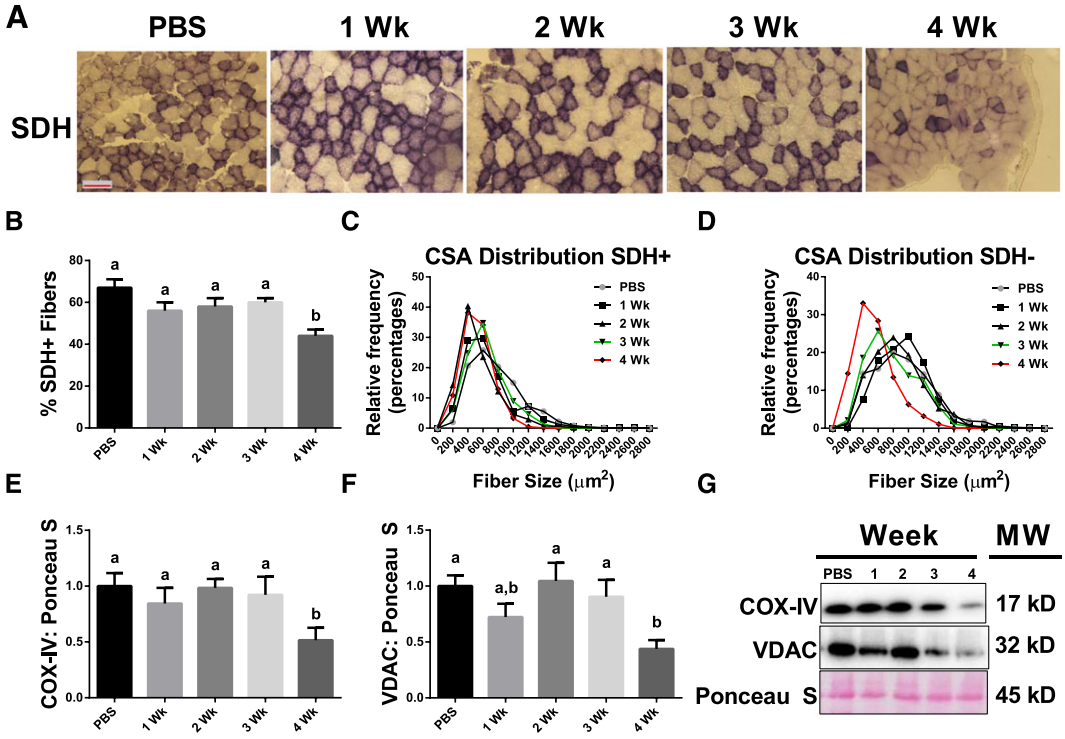

DOI: 10.1002/jcsm.12232

Mitochondrial degeneration occurs before cancer cachexia

Mitochondrial network degeneration is evident 2 weeks following tumour implantation. Examining the MitoTimer fluorescence spectra, we observed a ~50% and 4-fold greater MitoTimer red:green ratio and number of pure red puncta, respectively (*Figure* 3A–C). These measures were previously validated by Laker *et al.*[15] to directly indicate impaired mitochondrial quality. Furthermore, mitochondrial function (indicated by the RCR, the ratio of state 3:state 4 respiration) was ~25 and 45% lower 3 and 4 weeks following tumour implantation compared with PBS (*Figure* 3D). Moreover, mitochondrial ROS production, indicated by H_2O_2 emission, was 2-fold greater 1 week following tumour implantation and remained elevated through 3 weeks post-tumour implantation compared with PBS (*Figure* 3E).

Lewis lung carcinoma impairs mitochondrial quality control before development of cancer cachexia

Lewis lung carcinoma implantation did not affect the mitochondrial biogenesis proteins PGC-1α, PPARα, or TFAM; however, 1 week following tumour implantation, PPARδ protein content was ~40% lower compared with PBS, but not significantly different from control in other experimental groups (2–4 weeks post-tumour implantation) (*Figure* 4A and 4B). Mitochondrial dynamics was dysregulated as soon as 1 week following tumour implantation. Opa1 (a protein critical for mitochondrial inner membrane fusion) content was ~45% lower than PBS control in all LLC tumour-bearing groups (*Figure* 4C and 4D). Intriguingly, mitochondrial fission proteins Drp1 and Fis1 were differentially expressed throughout the progression of cancer cachexia. Drp1 protein

Figure 3 Mitochondrial degeneration precedes muscle wasting in cancer cachexia in Lewis lung carcinoma tumour-bearing mice. MitoTimer is a mitochondrially targeted variant of DsRed validated by Laker *et al.*[15] to emit green fluorescence when mitochondria are healthy and shift to red when mitochondria are damaged. (A–C) MitoTimer in FDB muscle. (A) Representative MitoTimer images taken at ×100 magnification. Scale bar is 20 μM in length. (B) Quantification of MitoTimer red:green ratio. (C) Quantification of pure red puncta in MitoTimer. Locations of pure red puncta co-localize with LC3 and appear to represent completely degenerated mitochondria targeted for autophagy.[15] (D–E) Mitochondrial function and ROS emission in plantaris muscle. (D) Respiratory control ratio (ratio of state 3:state 4 respiration) of permeabilized plantaris muscle. (E) Mitochondrial H_2O_2 production in permeabilized plantaris muscle. *N* of 12–24 per group was utilized for MitoTimer, while *N* of 12/group was utilized for respiration and ROS production analysis. Lettering denotes statistical significance at an alpha set at $P < 0.05$.

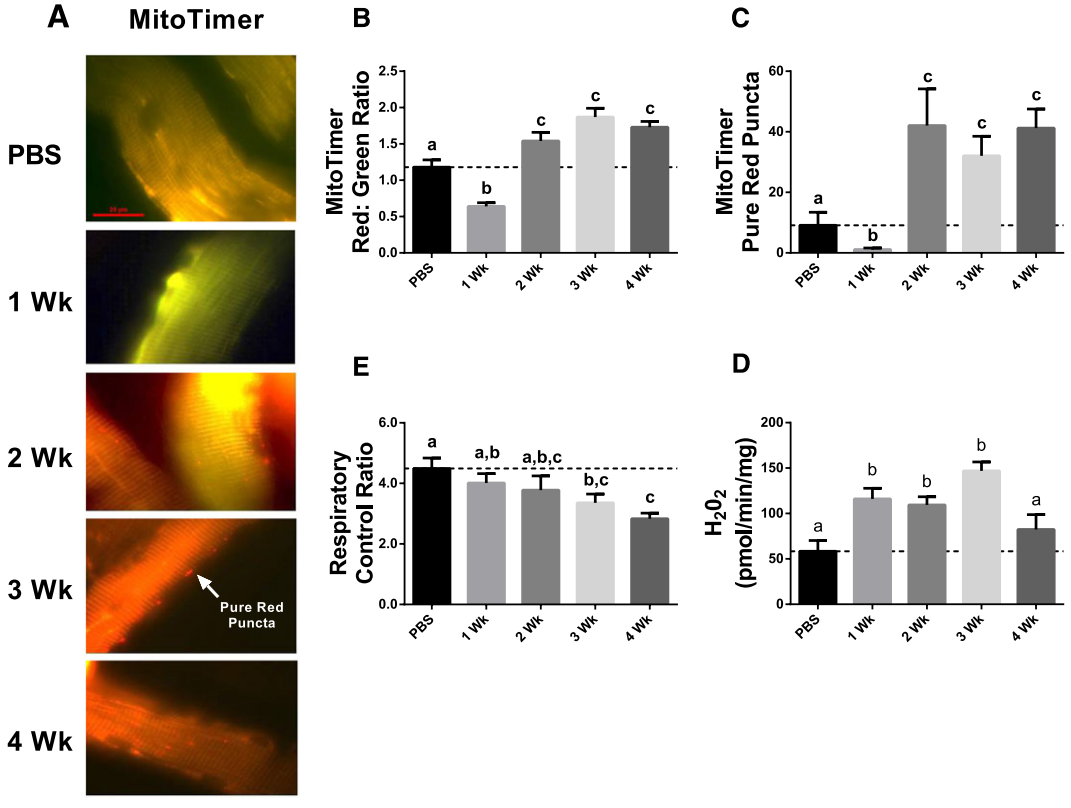

DOI: 10.1002/jcsm.12232

Figure 4 Immunoblot analysis of mitochondrial quality control regulators during progression of cancer cachexia in gastrocnemius muscle of Lewis lung carcinoma tumour-bearing mice. (A, B) Immunoblot quantification (A) and representative immunoblots (B) of mitochondrial biogenesis regulators PGC-1α, PPARα, PPARδ, and TFAM. (C, D) Immunoblot quantification (C) and representative immunoblots (D) of mitochondrial dynamic regulators MFN1, MFN2, OPA1, DRP1, and Fis1. (E, F) Immunoblot quantification (E) and representative immunoblots (F) of mitophagy regulators BNIP3, PINK1, p-PARKIN, and PARKIN. *N* of 7–8 per group was utilized for immunoblot analysis. Lettering denotes statistical significance at an alpha set at $P < 0.05$.

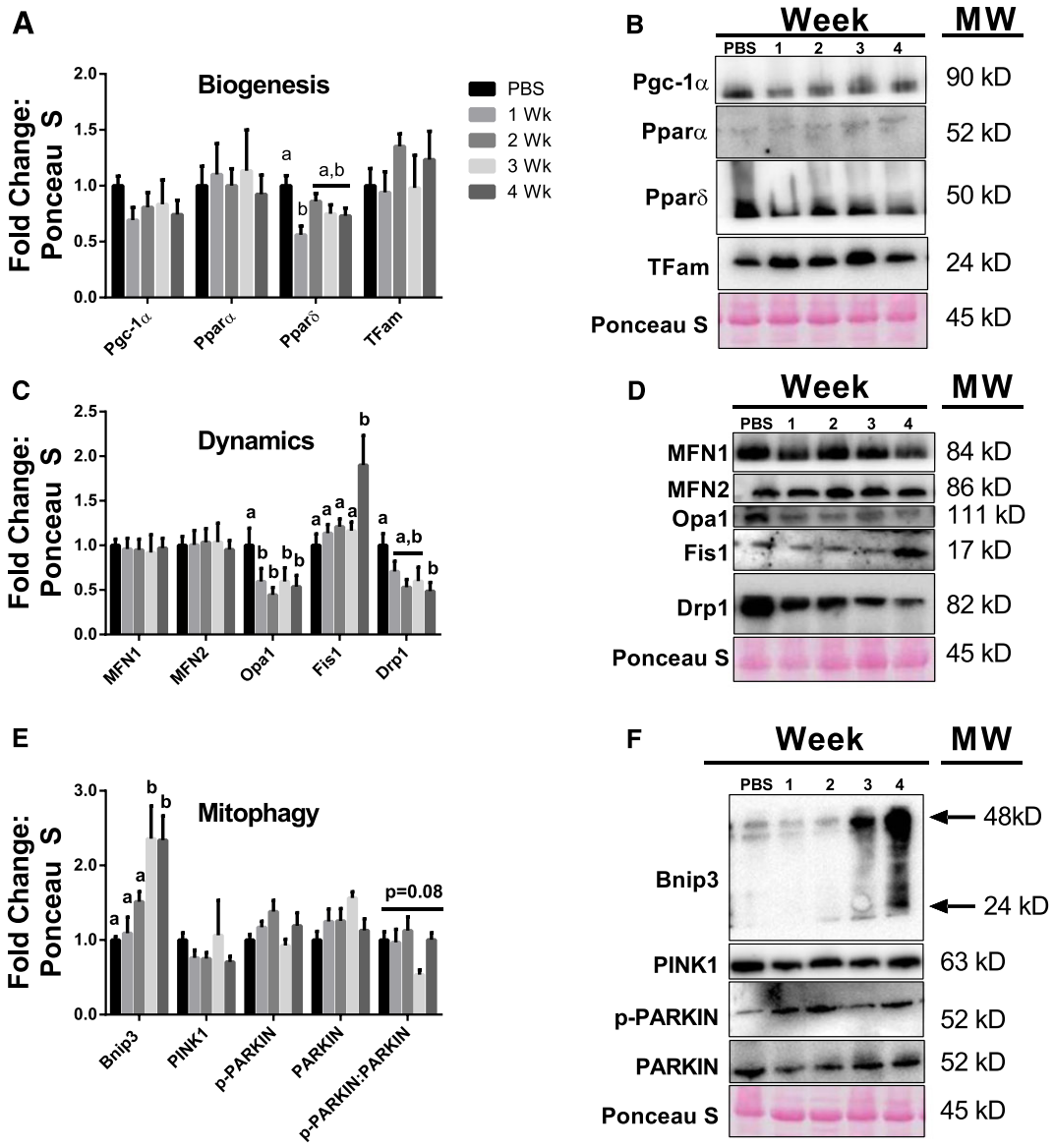

content was ~45% lower 4 weeks following tumour implantation compared with PBS; an apparent lower Drp1 content in 1–3 week tumour groups did not reach significance (*Figure* 4C and 4D). In contrast, Fis1 protein content was elevated ~80% in 4 week cachectic animals compared with PBS only (*Figure* 4C and 4D). Mitophagy regulator BNIP3 protein content was ~2-fold greater in 3 weeks following tumour implantation compared with PBS (*Figure* 4E and 4F). In contrast, PINK1, p-PARKIN, and PARKIN protein content were not significantly different among groups (*Figure* 4E and 4F).

Antioxidant enzymes are unchanged despite increased mitochondrial ROS production

Protein contents of SOD1, SOD2, SOD3, GPx3, GPx7, and catalase were not different among experimental groups (*Figure* 5).

Discussion

Current literature is clear that mitochondria are dysregulated in cachectic skeletal muscle.[25,32,45] However, our findings are

DOI: 10.1002/jcsm.12232

Figure 5 Content of antioxidant enzymes during progression of cancer cachexia in gastrocnemius muscle of Lewis lung carcinoma tumour-bearing mice. (A) Representative images of antioxidant enzymes. No statistically significant findings were found. *N* of 7–8 per group was utilized for immunoblot analysis.

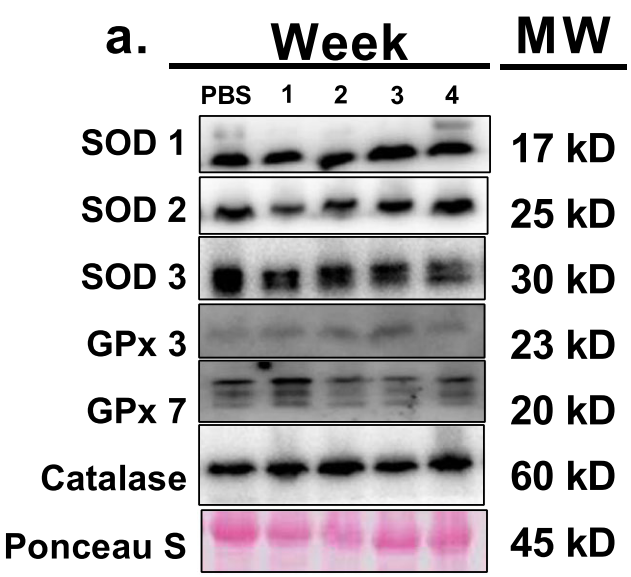

the first to demonstrate mitochondrial network deterioration, and dysfunction occurs before the onset of cancer-induced loss of muscle mass in tumour-bearing mice. Recently, mitochondria have been implicated as critical controllers of skeletal muscle mass[46]; therefore, mitochondrial degeneration may be a key promoter of cancer cachexia. Initial observations presented here and by White *et al.*[25] compared mitochondrial quality control regulators across degrees of cachexia in $Apc^{Min/+}$ mice suggesting that impaired mitochondrial quality precedes cachectic phenotype which have herein been built upon via time course and functional assessments in LLC tumour-bearing mice. The current study demonstrates increased mitochondrial oxidative stress within the muscle 1 week post-tumour implantation, followed by mitochondrial network degeneration and lost mitochondrial function 2 and 3 weeks post-tumour implantation, respectively. Moreover, mitochondrial quality control regulators are altered throughout the progression of cancer cachexia in both $Apc^{Min/+}$ and LLC pre-clinical models suggesting that early mitochondrial degenerations are a common alteration in the development of muscle wasting in cancer cachexia across pre-clinical models. Our findings clearly present functional mitochondrial degeneration as an early event preceding muscle wasting in the development of cancer cachexia in both LLC tumour-bearing and $Apc^{Min/+}$ mice. Furthermore, to our knowledge, we are the first to examine progression of cancer cachexia by time course design. The data presented herein demonstrate the imperative nature to elucidate intramyofibrillar alterations prior to the onset of the cachectic phenotype.

Cancer cachexia alters mitochondrial quality control signalling in $Apc^{Min/+}$ mice

In our examination of the $Apc^{Min/+}$ mouse, we note that mRNA contents of regulators of mitochondrial biogenesis (*Pgc-1α* and *Pparα*) and fusion (*Mfn2*) occur in the MinStable condition, that is, in tumour-bearing mice who do not present signs of the cachectic phenotype. In contrast, the mRNA content of mitophagy marker *Bnip3* was elevated only in cachectic mice. These signalling data are similar to White *et al.*[25] and suggested that mitochondrial quality control is impaired prior to signs of cachexia beginning with down-regulations of biogenic and fusion regulators and progressing to elevated markers of mitophagy in cachectic mice. Considering these data, we next elected to tease the mitochondrial degenerations in progression of cancer cachexia-induced muscle wasting using a tumour implantation model (LLC) to allow time course assessments of the functional mitochondrial alterations in development of this condition.

Cancer cachexia impairs oxidative phenotype and mitochondrial content in skeletal muscle in Lewis lung carcinoma tumour-bearing mice

Using this model (1×10^6 LLC cells implanted into the hind flank) of LLC-induced cancer cachexia, it takes 4 weeks for the cachectic phenotype (muscle wasting) to develop.[36,37,47] While our mice did not lose total body weight after 4 weeks following tumour implantation, significant muscle and fat mass was lost along with an increased spleen mass indicative of an inflammatory state,[48] which is an effective diagnostic criteria.[6] Loss of oxidative phenotype in late-stage cancer cachexia has commonly been observed in the literature[13,25,49]; however, oxidative phenotype throughout the progression of cancer cachexia is understudied. Our data indicate that loss of oxidative phenotype (SDH stain) and mitochondrial content (COX-IV/VDAC) occurs concomitantly with cancer-induced muscle loss. Furthermore, when cancer cachexia develops, our data indicate that oxidative muscle fibres may be resistant to atrophy during the initial stages of wasting (CSA distribution by SDH stain). Based on our data and prior reports, cancer cachexia preferentially impacts glycolytic muscle fibres; however, oxidative fibres have superior antioxidant defences when compared with glycolytic fibres,[50,51] which may slow cancer cachexia. This is commonly observed in cancer cachexia literature[49] and indicates that oxidative metabolism is an important factor for the maintenance of muscle size. Therefore, muscle mitochondria may be a

DOI: 10.1002/jcsm.12232

primary target of the cancer environment and may be a contributor to cancer-induced muscle wasting.[13]

Mitochondrial degeneration occurs prior to the onset of cancer-induced muscle loss

To determine functional mitochondrial degeneration, we examined multiple functional parameters including respiratory function, ROS emission, and fluorescence-based measures of network degeneration. We measured a 2-fold increase in ROS production 1 week post-tumour implantation. Chronically elevated ROS may be an instigating factor for the muscle wasting observed in tumour-bearing mice as it has been shown to promote protein catabolic functions.[16,17] We do note that mitochondrial ROS production appeared to normalize at 4 week post-tumour implantation; however, these data are normalized to tissue mass, and it must also be noted that at this time point, mitochondrial density is ~50% reduced by COX-IV and VDAC markers. Next, utilizing the reporter pMitotimer,[15] we observed signs of network degeneration 2 weeks following tumour implantation along with the sudden and dramatic appearance of pure red puncta which by prior reports appear to be completely degenerated mitochondria tagged for autophagic degradation.[15] Degeneration of the mitochondrial network then leads to impaired mitochondrial respiratory function, which we observed 3 weeks following tumour implantation. These combined findings suggest early and progressive derangements in mitochondrial health during the development of cancer cachexia in tumour-bearing mice (*Figure* 6).

The mitochondrial aberrations described herein may induce LLC-mediated cancer cachexia considering that damaged mitochondria have been shown to directly promote atrophic signalling in skeletal muscle in other models.[21–24] Furthermore, cellular energy stress induced by mitochondrial dysfunction leads to skeletal muscle wasting.[52] Our data demonstrate clear evidence that mitochondrial degeneration occurs before the development of cancer-induced muscle wasting in tumour-bearing mice. Critically, these aberrations are most likely due to influences of the tumour microenvironment as mitochondrial disruptions are observed only 1 week following tumour implant when the animal presents as otherwise healthy.

To provide insight to how these mitochondrial derangements occur, we next examined mechanisms of the mitochondrial quality control system in the LLC mice as mitochondrial degeneration observed in cancer-induced muscle wasting may be attributed to disruptions to these processes. While not all measured markers of mitochondrial quality control were altered, we note that when impacts were observed in mitochondrial biogenic (PPARδ) and fusion (Opa1) proteins, these alterations were via down-regulation and occurred shortly after tumour implantation (1 week). Intriguingly, $Apc^{Min/+}$ mice exhibit a significant reduction in *Pgc-1α* mRNA content in MinStable mice, while PGC-1α protein content is not altered throughout the progression of cancer cachexia in the LLC pre-clinical model. This may be explained by differences in the tumour microenvironment between the pre-clinical models. Moreover, *Pgc-1α* mRNA content is not different between MinCC and B6 control. At this time, we are unable to be certain as the reason behind reduced *Pgc-1α* mRNA in MinStable mice; however, differences in the inflammatory environment between the MinStable and MinCC group may explain this[53]; however, this is only speculative. Similar to $Apc^{Min/+}$ mice, in LLC mice, the mitochondrial fission regulator Fis1 and mitophagy protein BNIP3 were both met with induced expression and both only impacted later in cachectic development. These observations in mitochondrial quality control are similar to those presented here in the $Apc^{Min/+}$ mouse, and congruent with prior literature in cancer cachexia,[32] whereby early down-regulations in biogenic and fusion regulators followed by strong induction of *Bnip3* content is observed. These combined data suggest early stage mitochondrial degeneration as a commonality in two otherwise distinct pre-clinical models of cancer cachexia.

These observations may directly tie to the development of cachectic wasting. First, Opa1 has recently been identified as a key controller of muscle size.[54] Second, the induction of Fis1 suggests an up-regulation in the amount of fragmented mitochondria, which are typically inefficient at generating ATP[55] leading to cellular energy stress and loss of muscle mass. Furthermore, a decrease in content of these controllers of mitochondrial dynamics may indicate alterations in the balance of fusion and fission of the mitochondria.[56] Finally, mitophagy is regulated by two distinct processes: BNIP3-mediated mitophagy and PINK1-PARKIN-mediated

Figure 6 Summary of functional mitochondrial derangements preceding cachectic muscle wasting in tumour-bearing mice.

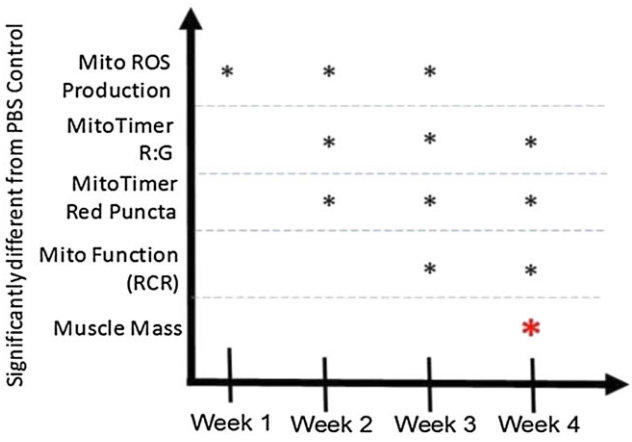

DOI: 10.1002/jcsm.12232

mitophagy.[57,58] While we have observed induction of BNIP3, such an impact on PINK1-PARKIN expression was not seen. This suggests differential regulation of BNIP3 compared with PINK1-PARKIN whereby alterations present in cancer cachexia selectively induce BNIP3-mediated mitophagy.

Considering the 2-fold increase of mitochondrial ROS production and the shift in MitoTimer fluorescence spectra, we next examined how cellular antioxidant defence mechanisms might be impacted in the development of cancer cachexia. Multiple lines of evidence suggest that excess ROS induces skeletal muscle atrophy.[59–64] Intriguingly, we examined protein contents of six antioxidant components all of which are unchanged despite an increase in mitochondrial ROS production, suggesting a failure of the system to adequately respond to mitochondrial oxidative stress which may exacerbate free radical-induced proteolysis during cancer cachexia. Unfortunately, we were unable to perform functional enzyme activity assays of antioxidant proteins to further elucidate the cellular response to oxidative stress due to lack of tissue. Further experiments should be performed to test these enzymatic activities to determine any alterations in function of antioxidant proteins.

Relationship between mitochondrial degeneration and cancer cachexia

Mitochondrial degeneration is a common feature across numerous models of skeletal muscle atrophy,[12,65,66] including cancer cachexia. In fact, mitochondrial degeneration may instigate skeletal muscle atrophy through mechanisms including reduced protein synthesis, increased autophagic and ubiquitin-proteasome-mediated protein catabolism, inflammation, and altered myogenesis all of which are perturbed in cancer cachexia.[18–24] In this study, we have clearly shown aberrations in the mitochondrial network, beginning with increased ROS production and leading to loss of mitochondrial function in cancer cachexia (*Figure* 6). Intriguingly, these alterations occur before cancer-induced loss of muscle mass occurs (*Figure* 6), and while animals would otherwise appear healthy suggesting mitochondrial degeneration in cancer cachexia is largely resultant of the tumour microenvironment. Functional data presented herein across time course with LLC-induced muscle wasting coupled with signalling data presented from the $Apc^{Min/+}$ and LLC experiments suggest that early onset mitochondrial degeneration is likely a common factor in the development of cancer-induced muscle loss across pre-clinical models which otherwise display distinct mechanistic traits.

Conclusions and future direction

In summary, this is the first experiment to investigate mitochondrial degeneration and dysfunction throughout a time course development of cancer cachexia in tumour-bearing mice. While altered signalling of mitochondrial regulatory processes (biogenesis, dynamics, and mitophagy) provides important insight into potential mechanisms behind mitochondrial degeneration, the current study directly measures mitochondrial quality (MitoTimer), mitochondrial ROS emission, and respiratory function (RCR) in order to fully assess mitochondrial aberrations that occur throughout the progression of cancer cachexia in a pre-clinical model. Intriguingly, mitochondrial aberrations such as increased ROS production occur as soon as 1 week after tumour implantation (*Figure* 6), which is likely instigated by the tumour microenvironment; however, at this time, we cannot rule out denervation, hypoxia, and/or apoptosis. Data from the current study implicate the importance of early cancer detection as well as preventive measures for cancer cachexia. However, cancer cachexia is often not treated before stage IV of cancer is reached.[67] These data suggest that targeting of mitochondrial quality may be vital for the treatment and prevention of cancer cachexia whether pharmacologically or through exercise.[15,28] Although future studies will need to validate promotion of mitochondrial quality as an efficacious modality. To accomplish this, future experiments should be performed to determine if promoting maintenance of mitochondrial quality may prevent cancer-induced muscle wasting. We now see a clear need for further study of the early stage progression of cancer cachexia as well as early stage impacts of the tumour microenvironment.

Acknowledgements

Support for LLC experiments has been provided in part by the Arkansas Biosciences Institute, the major research component of the Arkansas Tobacco Settlement Proceeds Act of 2000 and by the National Institutes of Health under Award Number R15AR069913 from the National Institute Of Arthritis And Musculoskeletal And Skin Diseases and the National Institute Of General Medical Sciences (NPG). $Apc^{Min/+}$ experiments were partially supported by National Institutes of Health grant no. R01CA121249A501 (JAC) from the National Cancer Institute and the National Institutes of Health grant no. 5P30GM103336 from the National Institute of General Medicine. Contents of this publication are solely the responsibility of the authors and do not necessarily represent the official views of the ABI, NIGMS, or NIH. The authors would like to thank Drs Sami Dridi, Elizabeth Greene and Jeffrey Wolchok (U. Arkansas), as well as Mr Dennis Fix (U. S. Carolina), Mr Connor Benson (UT Tyler), Ms Haley McCarver, and Mr Aaron Caldwell for their contributions to the experiments presented here and editing. We would like to thank the Cell and Molecular Biology program at the University of Arkansas, Fayetteville for supporting Jacob L. Brown's graduate education. We would also like to extend our gratitude to the numerous other faculty, staff, and students of the Integrative Muscle Biology

Laboratory at the University of South Carolina and the Exercise Science Research Center at the University of Arkansas.

The authors certify that they comply with the ethical guidelines for publishing in the Journal of Cachexia, Sarcopenia, and Muscle.[68]

Conflict of interest

None declared.

References

1. Ferlay J, Soerjomataram I, Dikshit R, Eser S, Mathers C, Rebelo M, et al. Cancer incidence and mortality worldwide: sources, methods and major patterns in GLOBOCAN 2012. *Int J Cancer* 2015;**136**:E359–E386.
2. Fitzmaurice C, Dicker D, Pain A, Hamavid H, Moradi-Lakeh M, MacIntyre MF, et al. The Global Burden of Cancer 2013. *JAMA Oncol* 2015;**1**:505–527.
3. Jemal A, Ward E, Hao Y, Thun M. Trends in the leading causes of death in the United States, 1970-2002. *JAMA* 2005;**294**:1255–1259.
4. Fearon Kenneth CH, Glass David J, Guttridge DC. Cancer cachexia: mediators, signaling, and metabolic pathways. *Cell Metab* 2012;**16**:153–166.
5. Onesti JK, Guttridge DC. Inflammation based regulation of cancer cachexia. *Biomed Res Int* 2014;**2014**:168407.
6. Fearon K, Strasser F, Anker SD, Bosaeus I, Bruera E, Fainsinger RL, et al. Definition and classification of cancer cachexia: an international consensus. *Lancet Oncol* 2011;**12**:489–495.
7. Fearon K. Cachexia: Treat wasting illness on multiple fronts. *Nature* 2016;**529**:156.
8. Baltgalvis KA, Berger FG, Peña MMO, Davis JM, White JP, Carson JA. Muscle wasting and interleukin-6-induced atrogin-I expression in the cachectic Apc(Min/+) mouse. *Pflugers Archiv : European journal of physiology* 2009;**457**:989–1001.
9. Li P, Waters RE, Redfern SI, Zhang M, Mao L, Annex BH, et al. Oxidative phenotype protects myofibers from pathological insults induced by chronic heart failure in mice. *Am J Pathol* 2007;**170**:599–608.
10. Yu Z, Li P, Zhang M, Hannink M, Stamler JS, Yan Z. Fiber type-specific nitric oxide protects oxidative myofibers against cachectic stimuli. *PLoS One* 2008;**3**: e2086.
11. Acharyya S, Ladner KJ, Nelsen LL, Damrauer J, Reiser PJ, Swoap S, et al. Cancer cachexia is regulated by selective targeting of skeletal muscle gene products. *J Clin Invest* 2004;**114**:370–378.
12. Kandarian SC, Jackman RW. Intracellular signaling during skeletal muscle atrophy. *Muscle Nerve* 2006;**33**:155–165.
13. Carson JA, Hardee JP, VanderVeen BN. The emerging role of skeletal muscle oxidative metabolism as a biological target and cellular regulator of cancer-induced muscle wasting. *Semin Cell Dev Biol* 2016;**54**:53–67.
14. Greene NP, Lee DE, Brown JL, Rosa ME, Brown LA, Perry RA, et al. Mitochondrial quality control, promoted by PGC-1alpha, is dysregulated by Western diet-induced obesity and partially restored by moderate physical activity in mice. *Physiol Rep* 2015;**3**:e12470.
15. Laker RC, Xu P, Ryall KA, Sujkowski A, Kenwood BM, Chain KH, et al. A novel MitoTimer reporter gene for mitochondrial content, structure, stress, and damage in vivo. *J Biol Chem* 2014;**289**:12005–12015.
16. Anderson EJ, Lustig ME, Boyle KE, Woodlief TL, Kane DA, Lin CT, et al. Mitochondrial H2O2 emission and cellular redox state link excess fat intake to insulin resistance in both rodents and humans. *J Clin Invest* 2009;**119**:573–581.
17. Koves TR, Ussher JR, Noland RC, Slentz D, Mosedale M, Ilkayeva O, et al. Mitochondrial overload and incomplete fatty acid oxidation contribute to skeletal muscle insulin resistance. *Cell Metab* 2008;**7**:45–56.
18. Cannavino J, Brocca L, Sandri M, Bottinelli R, Pellegrino MA. PGC1-alpha overexpression prevents metabolic alterations and soleus muscle atrophy in hindlimb unloaded mice. *J Physiol* 2014;**592**:4575–4589.
19. Ji LL. Redox signaling in skeletal muscle: role of aging and exercise. *Adv Physiol Educ* 2015;**39**:352–359.
20. Bijland S, Mancini SJ, Salt IP. Role of AMP-activated protein kinase in adipose tissue metabolism and inflammation. *Clin Sci (Lond)* 2013;**124**:491–507.
21. Debold EP. Potential molecular mechanisms underlying muscle fatigue mediated by reactive oxygen and nitrogen species. *Frontiers in physiology* 2015;**6**:239.
22. Lamb GD, Westerblad H. Acute effects of reactive oxygen and nitrogen species on the contractile function of skeletal muscle. *J Physiol* 2011;**589**:2119–2127.
23. Sivakumar AS, Hwang I. Effects of Sunphenon and Polyphenon 60 on proteolytic pathways, inflammatory cytokines and myogenic markers in H2O2-treated C2C12 cells. *J Biosci* 2015;**40**:53–59.
24. Liu J, Peng Y, Wang X, Fan Y, Qin C, Shi L, et al. Mitochondrial dysfunction launches dexamethasone-induced skeletal muscle atrophy via AMPK/FOXO3 signaling. *Mol Pharm* 2016;**13**:73–84.
25. White JP, Baltgalvis KA, Puppa MJ, Sato S, Baynes JW, Carson JA. Muscle oxidative capacity during IL-6-dependent cancer cachexia. *Am J Physiol Regul Integr Comp Physiol* 2011;**300**:R201–R211.
26. Sullivan-Gunn MJ, Campbell-O'Sullivan SP, Tisdale MJ, Lewandowski PA. Decreased NADPH oxidase expression and antioxidant activity in cachectic skeletal muscle. *J Cachexia Sarcopenia Muscle* 2011;**2**:181–188.
27. Velazquez KT, Enos RT, Narsale AA, Puppa MJ, Davis JM, Murphy EA, et al. Quercetin supplementation attenuates the progression of cancer cachexia in ApcMin/+ mice. *J Nutr* 2014;**144**:868–875.
28. Yan Z, Lira VA, Greene NP. Exercise training-induced regulation of mitochondrial quality. *Exerc Sport Sci Rev* 2012;**40**:159–164.
29. Puigserver P, Wu Z, Park CW, Graves R, Wright M, Spiegelman BM. A cold-inducible coactivator of nuclear receptors linked to adaptive thermogenesis. *Cell* 1998;**92**:829–839.
30. Jin SM, Youle RJ. PINK1- and Parkin-mediated mitophagy at a glance. *J Cell Sci* 2012;**125**:795–799.
31. Lemasters JJ. Selective mitochondrial autophagy, or mitophagy, as a targeted defense against oxidative stress, mitochondrial dysfunction, and aging. *Rejuvenation Res* 2005;**8**:3–5.
32. White JP, Puppa MJ, Sato S, Gao S, Price RL, Baynes JW, et al. IL-6 regulation on skeletal muscle mitochondrial remodeling during cancer cachexia in the ApcMin/+ mouse. *Skeletal muscle* 2012;**2**:14.
33. Cannavino J, Brocca L, Sandri M, Grassi B, Bottinelli R, Pellegrino MA. The role of alterations in mitochondrial dynamics and PGC-1alpha over-expression in fast muscle atrophy following hindlimb unloading. *J Physiol* 2015;**593**:1981–1995.
34. Powers SK, Wiggs MP, Duarte JA, Zergeroglu AM, Demirel HA. Mitochondrial signaling contributes to disuse muscle atrophy. *Am J Physiol Endocrinol Metab* 2012;**303**:E31–E39.
35. Kuo YT, Shih PH, Kao SH, Yeh GC, Lee HM. Pyrroloquinoline quinone resists

denervation-induced skeletal muscle atrophy by activating PGC-1alpha and integrating mitochondrial electron transport chain complexes. *PLoS One* 2015;**10**: e0143600.

36. Lee DE, Brown JL, Rosa-Caldwell ME, Blackwell TA, Perry RA Jr, Brown LA, et al. Cancer cachexia-induced muscle atrophy: evidence for alterations in microRNAs important for muscle size. *Physiol Genomics* 2017;https://doi.org/10.1152/physiolgenomics.00006.2017.
37. Puppa MJ, Gao S, Narsale AA, Carson JA. Skeletal muscle glycoprotein 130's role in Lewis lung carcinoma-induced cachexia. *FASEB journal: official publication of the Federation of American Societies for Experimental Biology* 2014;**28**:998–1009.
38. Min K, Kwon O-S, Smuder AJ, Wiggs MP, Sollanek KJ, Christou DD, et al. Increased mitochondrial emission of reactive oxygen species and calpain activation are required for doxorubicin-induced cardiac and skeletal muscle myopathy. *J Physiol* 2015;**593**:2017–2036.
39. Brown LA, Lee DE, Patton JF, Perry RA, Brown JL, Baum J, et al. Diet-induced obesity alters anabolic signaling in mice at the onset of muscle regeneration. *Acta Physiologica* 2015; **215**:46–57.
40. Lee DE, Brown JL, Rosa ME, Brown LA, Perry RA Jr, Washington TA, et al. Translational machinery of mitochondrial mRNA is promoted by physical activity in Western diet-induced obese mice. *Acta Physiol (Oxf)* 2016; **218**:167–177.
41. Brown JL, Rosa-Caldwell ME, Lee DE, Brown LA, Perry RA, Shimkus KL, et al. PGC-1alpha4 gene expression is suppressed by the IL-6-MEK-ERK 1/2 MAPK signalling axis and altered by resistance exercise, obesity and muscle injury. *Acta Physiol (Oxf)* 2016; **220**:275–288.
42. Rosa-Caldwell ME, Lee DE, Brown JL, Brown LA, Perry RA Jr, Greene ES, et al. Moderate physical activity promotes basal hepatic autophagy in diet-induced obese mice. *Applied physiology, nutrition, and metabolism = Physiologie appliquee, nutrition et metabolisme* 2017;**42**:148–156.
43. Perry RA Jr, Brown LA, Lee DE, Brown JL, Baum JI, Greene NP, et al. Differential effects of leucine supplementation in young and aged mice at the onset of skeletal muscle regeneration. *Mech Ageing Dev* 2016;**157**:7–16.
44. Powers SK, Lennon SL. Analysis of cellular responses to free radicals: focus on exercise and skeletal muscle. *Proc Nutr Soc* 1999;**58**:1025–1033.
45. Constantinou C, Fontes De Oliveira CC, Mintzopoulos D, Busquets S, He J, Kesarwani M, et al. Nuclear magnetic resonance in conjunction with functional genomics suggests mitochondrial dysfunction in a murine model of cancer cachexia. *Int J Mol Med* 2011;**27**:15–24.
46. Romanello V, Sandri M. Mitochondrial biogenesis and fragmentation as regulators of muscle protein degradation. *Curr Hypertens Rep* 2010;**12**:433–439.
47. Pin F, Busquets S, Toledo M, Camperi A, Lopez-Soriano FJ, Costelli P, et al. Combination of exercise training and erythropoietin prevents cancer-induced muscle alterations. *Oncotarget* 2015;**6**:43202–43215.
48. Anderson LJ, Albrecht ED, Garcia JM. Update on management of cancer-related cachexia. *Curr Oncol Rep* 2017;**19**:3.
49. Ciciliot S, Rossi AC, Dyar KA, Blaauw B, Schiaffino S. Muscle type and fiber type specificity in muscle wasting. *Int J Biochem Cell Biol* 2013;**45**:2191–2199.
50. Charles AL, Guilbert AS, Guillot M, Talha S, Lejay A, Meyer A, et al. Muscles susceptibility to ischemia-reperfusion injuries depends on fiber type specific antioxidant level. *Frontiers in physiology.* 2017;**8**:52.
51. Okutsu M, Call JA, Lira VA, Zhang M, Donet JA, French BA, et al. Extracellular superoxide dismutase ameliorates skeletal muscle abnormalities, cachexia, and exercise intolerance in mice with congestive heart failure. *Circ Heart Fail* 2014;**7**:519–530.
52. Max SR. Disuse atrophy of skeletal muscle: loss of functional activity of mitochondria. *Biochem Biophys Res Commun* 1972;**46**:1394–1398.
53. White JP, Baynes JW, Welle SL, Kostek MC, Matesic LE, Sato S, et al. The regulation of skeletal muscle protein turnover during the progression of cancer cachexia in the Apc(Min/+) mouse. *PLoS One* 2011;**6**: e24650.
54. Varanita T, Soriano Maria E, Romanello V, Zaglia T, Quintana-Cabrera R, Semenzato M, et al. The Opa1-dependent mitochondrial cristae remodeling pathway controls atrophic, apoptotic, and ischemic tissue damage. *Cell Metab* 2015;**21**:834–844.
55. Benard G, Bellance N, James D, Parrone P, Fernandez H, Letellier T, et al. Mitochondrial bioenergetics and structural network organization. *J Cell Sci* 2007;**120**:838–848.
56. Wada J, Nakatsuka A. Mitochondrial dynamics and mitochondrial dysfunction in diabetes. *Acta Med Okayama* 2016;**70**:151–158.
57. Pickrell AM, Youle RJ. The roles of PINK1, parkin, and mitochondrial fidelity in Parkinson's disease. *Neuron* 2015;**85**:257–273.
58. Youle RJ, Narendra DP. Mechanisms of mitophagy. *Nat Rev Mol Biol* 2011;**12**:9–14
59. Appell HJ, Duarte JA, Soares JM. Supplementation of vitamin E may attenuate skeletal muscle immobilization atrophy. *Int J Sports Med* 1997;**18**:157–160.
60. Whidden MA, Smuder AJ, Wu M, Hudson MB, Nelson WB, Powers SK. Oxidative stress is required for mechanical ventilation-induced protease activation in the diaphragm. *Journal of applied physiology (Bethesda, Md: 1985)* 2010;**108**:1376–1382.
61. McClung JM, Judge AR, Talbert EE, Powers SK. Calpain-1 is required for hydrogen peroxide-induced myotube atrophy. *Am J Physiol Cell Physiol* 2009;**296**:C363–C371.
62. Powers SK, Morton AB, Ahn B, Smuder AJ. Redox control of skeletal muscle atrophy. *Free Radic Biol Med* 2016;**98**:208–217.
63. Li YP, Chen Y, Li AS, Reid MB. Hydrogen peroxide stimulates ubiquitin-conjugating activity and expression of genes for specific E2 and E3 proteins in skeletal muscle myotubes. *Am J Physiol Cell Physiol* 2003;**285**:C806–C812.
64. O'Loghlen A, Perez-Morgado MI, Salinas M, Martin ME. N-acetyl-cysteine abolishes hydrogen peroxide-induced modification of eukaryotic initiation factor 4F activity via distinct signalling pathways. *Cell Signal* 2006;**18**:21–31.
65. Reggiani C. Regulation of muscle mass: a new role for mitochondria? *J Physiol* 2015;**593**:1761–1762.
66. Borgia D, Malena A, Spinazzi M, Andrea Desbats M, Salviati L, Russell AP, et al. Increased mitophagy in the skeletal muscle of spinal and bulbar muscular atrophy patients. *Hum Mol Genet* 2017; **26**:1087–1103.
67. Muscaritoli M, Rossi Fanelli F, Molfino A. Perspectives of health care professionals on cancer cachexia: results from three global surveys. *Ann Oncol* 2016;**27**:2230–2236.
68. von Haehling S, Morley JE, Coats AJ, Anker SD. Ethical guidelines for publishing in the Journal of Cachexia, Sarcopenia and Muscle: update 2015. *J Cachexia Sarcopenia Muscle* 2015;**6**:315–316.